

# **<sup>124</sup>I PET Assessment of Response of Bone Metastases to Initial Radioiodine Treatment of Differentiated Thyroid Cancer**

Walter Jentzen<sup>1</sup>, Femke Verschure<sup>2</sup>, Annelie van Zon<sup>2</sup>, Rudie van de Kolk<sup>2</sup>, Roel Wierts<sup>3</sup>, Jochen Schmitz<sup>1</sup>, Andreas Bockisch<sup>1</sup>, and Ina Binse<sup>1</sup>

<sup>1</sup>Klinik für Nuklearmedizin, Universität Duisburg-Essen, Essen, Germany; <sup>2</sup>Fontys University of Applied Sciences, Eindhoven, The Netherlands; and <sup>3</sup>Maastricht University Medical Centre, Maastricht, The Netherlands

Iodine-positive bone metastases (BMs) are often resistant after initial radioiodine therapy applying the standard-activity approach. A comprehensive lesion-based response study for BMs has not, to our knowledge, yet been performed. In this study, pretherapy and follow-up <sup>124</sup>I PET/CT data on BMs from differentiated thyroid cancer patients were retrospectively analyzed to assess the relationship between absorbed dose (AD) of radiation and response after initial radioiodine treatment.

**Methods:** Before and after initial radioiodine therapy, patients underwent serial PET/CT scanning after administration of 20–40 MBq of <sup>124</sup>I. The pretherapy PET data were used to segment BM volumes and to predict the average ADs after administration of dosimetry-guided <sup>131</sup>I activity. The lower volume limit of determinability of the applied segmentation method was a sphere volume of 0.16 mL. This volume limit classified the BMs into known-volume and fixed-volume groups with their respective average and minimum ADs. Follow-up <sup>124</sup>I and <sup>18</sup>F-FDG PET/CT data after treatment were analyzed to assess lesion-based therapy response. Response rates at different AD thresholds were calculated and were expressed as the percentage of completely responding BMs above the respective AD threshold. BMs with a maximum extent greater than twice the PET spatial resolution were visually scored for nonuniformity. **Results:** In total, 61 BMs in 10 patients were included, of which 46 and 15 comprised the known-volume group and the fixed-volume group, respectively. The median follow-up time was 5.6 mo (range, 3.7–23.2 mo). The median average and median minimum ADs in therapy were 183 Gy (range, 39–3,600 Gy) and 270 Gy (range, 63–1,300 Gy), respectively. A range of response rate of 70%–80% was achieved at an AD threshold range of 350–650 Gy. There were 26 BMs that were amenable to visual assessment of nonuniformity, of which two thirds (17/26) were scored as clearly nonuniform, and the majority (11/17) of these nonuniform BMs responded incompletely. **Conclusion:** Both the high AD threshold associated with high response rates and the low median AD per unit of <sup>131</sup>I activity elucidate the difficulty in achieving therapeutic efficacy for BMs when a single standard activity is administered. The relatively high AD threshold range is possibly a result of distinct levels of spatial nonuniformity in ADs.

**Key Words:** thyroid carcinoma; dosimetry; <sup>124</sup>I; radioiodine therapy; bone metastases

**J Nucl Med** 2016; 57:1499–1504

DOI: 10.2967/jnumed.115.170571

**R**adioiodine therapy after total thyroidectomy has been established in the management of patients with differentiated thyroid cancer (1,2). Radioiodine therapy is used to ablate thyroid remnants and, primarily, to eliminate lymph node metastases (LMs) and distant metastases, most commonly pulmonary (PMs) and bone (BMs).

In performing radioiodine treatment, most institutions apply the standard-activity approach. In contrast, we perform an individual pretherapy dosimetry for high-risk patients using the positron-emitting tracer <sup>124</sup>I-NaI (<sup>124</sup>I). In this dosimetry approach, the lesion-absorbed radiation dose (AD) per unit of <sup>131</sup>I activity is estimated using <sup>124</sup>I PET/CT and the maximum tolerable activity is derived from blood sample and whole-body retention data (3,4). The maximum tolerable activity is defined as the maximum therapeutic activity that can be administered without producing severe bone marrow or lung toxicities (≥grade 3 according to the National Cancer Institute Common Terminology Criteria for Adverse Events, version 4.0). The dosimetry data are used to calculate an individual therapeutic activity that results in ADs higher than the accepted AD thresholds without exceeding the maximum tolerable therapeutic activity.

The widely accepted AD thresholds are approximately 85 Gy for metastatic tissue and 300 Gy for thyroid remnant tissue. These key quantities were derived more than 2 decades ago by Maxon et al. (5), who demonstrated a response rate of approximately 80%–90%. However, the historical data by Maxon et al. included cervical LMs but not distant metastases. Thus, pretherapy dosimetry studies implicitly assume that the widely accepted AD threshold is also valid for distant metastases, such as PMs and BMs. A recent lesion-based dose response study (3) using <sup>124</sup>I PET/CT demonstrated that the 85-Gy AD threshold may be valid for LMs and also for PMs, as a high response rate of more than 80% was observed. In contrast, after single standard <sup>131</sup>I activities, multiple studies (6–8) reported that iodine-positive BMs were often resistant after initial radioiodine therapy. To our knowledge, a comprehensive lesion-based response study for BMs has not yet been performed. We are aware of only 2 studies (3,9) that have assessed a lesion-based therapy response of BMs, with a total of 6 BMs exceeding the AD threshold of 85 Gy.

Since 2003, we have been routinely conducting pretherapy <sup>124</sup>I PET/CT dosimetry for high-risk thyroid cancer patients, a few of whom have received a second <sup>124</sup>I PET/CT dosimetry after radioiodine treatment as part of the follow-up examination. Thus, the aim of this retrospective <sup>124</sup>I PET/CT study was to assess the relationship between AD of BMs and response after initial radioiodine treatment.

Received Feb. 9, 2016; revision accepted Apr. 12, 2016.

For correspondence or reprints contact: Walter Jentzen, Klinik für Nuklearmedizin, Universität Duisburg-Essen, Hufelandstrasse 55, D-45122 Essen, Germany.

E-mail: walter.jentzen@uni-duisburg-essen.de

Published online May 19, 2016.

COPYRIGHT © 2016 by the Society of Nuclear Medicine and Molecular Imaging, Inc.

## MATERIALS AND METHODS

### Inclusion Criteria and Patient Preparation

The patients provided written informed consent to undergo the examination, and the study was approved by the local ethics committee. Patients who had undergone  $^{124}\text{I}$  PET/CT dosimetry before their first radioiodine therapy were included. After radioiodine treatment, the patients underwent follow-up examinations consisting of, minimally, a posttherapy  $^{124}\text{I}$  PET/CT scan and an  $^{18}\text{F}$ -FDG PET/CT scan. Patients were excluded if they had received any treatments, such as surgery, between the pretherapy and follow-up scans. BMs were included if they were unambiguously assigned as BMs. The BM had to be sufficiently separated from radioiodine-accumulating tissues to minimize spill-in of external activity into the BM.

Patient preparation was similar for the pretherapy and follow-up  $^{124}\text{I}$  PET/CT examinations. All patients had undergone total thyroidectomy. The patients were receiving either endogenous thyroid-stimulating hormone (TSH) stimulation (by levothyroxine withdrawal for 4 wk) or exogenous TSH stimulation (by use of recombinant human TSH), with TSH levels of at least 30 mIU/L. Exogenous TSH stimulation was performed if exacerbation of concomitant disease was expected. Recombinant human TSH administration was required for the pretherapy dosimetry and again for radioiodine therapy. The patients were instructed to be on a low-iodine diet for 4 wk before the  $^{124}\text{I}$  PET/CT scans. Iodine contamination was excluded by urine testing. The single therapeutic  $^{131}\text{I}$  activity was individually assessed by an expert team that considered the pretherapy results of all lesions as well as the results of the toxicity levels of the activity-limiting organs (10). The treatment activity was administered 1–2 d after the last pretherapy scan. The  $^{18}\text{F}$ -FDG PET/CT scans were performed to identify initially iodine-positive BMs that changed to vital  $^{18}\text{F}$ -FDG-positive ones after radioiodine therapy. Patients fasted for at least 4 h before undergoing  $^{18}\text{F}$ -FDG PET/CT. The measured blood glucose level at the time of tracer injection was below 150 mg/dL.

### Image Acquisition and Reconstruction

The images were acquired on a Biograph Duo PET/CT scanner (Siemens Medical Solutions). Two PET/CT scans (at 24 h and  $\geq 96$  h) were acquired after administration of 20–40 MBq of  $^{124}\text{I}$  for the pretherapy and follow-up investigations.  $^{18}\text{F}$ -FDG scans were acquired 55–70 min after injection of 300 MBq of  $^{18}\text{F}$ -FDG. The examinations included whole-body PET/CT scans from head to thigh using 5–8 bed positions. PET/CT started with a spiral CT scan acquired using low-dose technique (tube voltage of 110 kVp, tube current-time product of 15 mAs, pitch of 1.6, and slice width of 5 mm). No CT contrast agent was applied. The  $^{124}\text{I}$  and  $^{18}\text{F}$ -FDG PET emission time was 3–5 min per bed position.

The PET images were reconstructed after Fourier rebinning using iterative attenuation-weighted ordered-subset expectation maximization with 4 iterations and 16 subsets. A relatively small postreconstruction gaussian smoothing filter of 1 mm was applied to obtain a high reconstructed PET spatial resolution of 6.7 mm. Standard scatter, attenuation, and dead-time corrections provided by the manufacturer were used. The reconstructed transverse emission images had a voxel size of  $1.7 \times 1.7 \times 2.4$  mm $^3$ . Filtered backprojection using a reconstruction kernel B40s was applied for the CT images (voxel size of  $1.0 \times 1.0 \times 2.4$  mm $^3$ ).

### Volumetry and Categorization into 3 Volume Groups

The low-dose CT images for BM volume segmentation could have been used; however, discerning the BM was often difficult or not possible. To include all the BMs observed on pretherapy  $^{124}\text{I}$  PET images and to use a consistent methodology, an improved PET-based iterative thresholding method was applied to pretherapy 24-h  $^{124}\text{I}$  PET

images (11). The volume segmentation algorithm used the enclosed delineation-averaged activity concentration instead of the commonly used maximum signal. This volume segmentation method has been shown to segment tumors more reliably in the presence of nonuniform uptake than the maximum-based approach. The lower volume limit of determinability was a sphere-equivalent diameter equaling the PET spatial resolution (6.7 mm or 0.16 mL).

Three groups of BMs were considered in this study. The first group contained BMs that were amenable to reliable volume estimations ( $>0.16$  mL) and was termed the known-volume group. The second group included BMs with volumes no larger than 0.16 mL and was termed the fixed-volume group. (In a previous study (3), the second group was referred to as the small-volume group.) The third group was a subgroup of the first group and was termed the large-volume group. It comprised BMs that were large enough to be assessed visually for nonuniformity. A BM was considered large if its maximum 3-dimensional extent was greater than twice the PET spatial resolution; the maximum extent was obtained by measuring distances within the segmented BM image (11).

### AD Calculations

The AD calculations involved different steps, which have been described in previous studies (12,13). Average  $^{124}\text{I}$  activity concentrations were evaluated for BMs in the known-volume group. In the fixed-volume group, the average  $^{124}\text{I}$  activity concentration was ascertained using a spheric volume of interest with a fixed volume of 0.16 mL (3). In follow-up images, the volume often decreased below 0.16 mL; in that case, the fixed-volume activity concentration was used to estimate uptake.

Two corrections, partial-volume effect and half-life, were necessary to obtain the projected  $^{131}\text{I}$  activity concentrations and their uptake values, which were used to estimate the  $^{131}\text{I}$  residence time. Using the  $^{131}\text{I}$  uptake values at 24 h and at least 96 h, either a bi- or a triphasic model was used to estimate the residence time. When the effective  $^{131}\text{I}$  half-life was less than or equal to the physical  $^{131}\text{I}$  half-life, the residence time was estimated using the adapted 2-point approach (14). In this approach, the uptake curve was biphasic and was parameterized using a combination of a linear function and a monoexponential function. The uptake curve was parameterized with a triphasic model when the effective  $^{131}\text{I}$  half-life was greater than the physical  $^{131}\text{I}$  half-life. The residence time arising from the first and second phases was the time integral from zero to the last measured point using the functions based on the biphasic model. The contribution resulting from the third phase was calculated assuming physical decay after the last imaging time point.

The above procedures yielded average and minimum ADs per unit of  $^{131}\text{I}$  activity for the known-volume and fixed-volume groups, respectively; a common osseous tissue density of 1.3 g/mL was used for all BMs. The predicted average and minimum ADs in therapy were calculated using the single therapeutic activity administered to the patient.

The present dosimetry calculations assume a uniform AD distribution within the BM, which is often not true in reality. Moreover, the PET-based ADs were slightly higher than the actually delivered ADs because a more rapid  $^{131}\text{I}$  release is expected during therapy. In addition, the stunning effect, which may diminish the ADs in therapy, was not likely to have a significant impact on therapeutic efficacy because low  $^{124}\text{I}$  activities were used (15).

### Therapy Response Assessment and Response Rate

Each individual BM was defined as either completely or incompletely responding. A completely responding BM was negative on both  $^{124}\text{I}$  PET/CT and  $^{18}\text{F}$ -FDG PET/CT follow-up images. An incompletely responding BM showed conspicuous focal  $^{124}\text{I}$  or  $^{18}\text{F}$ -FDG uptake.

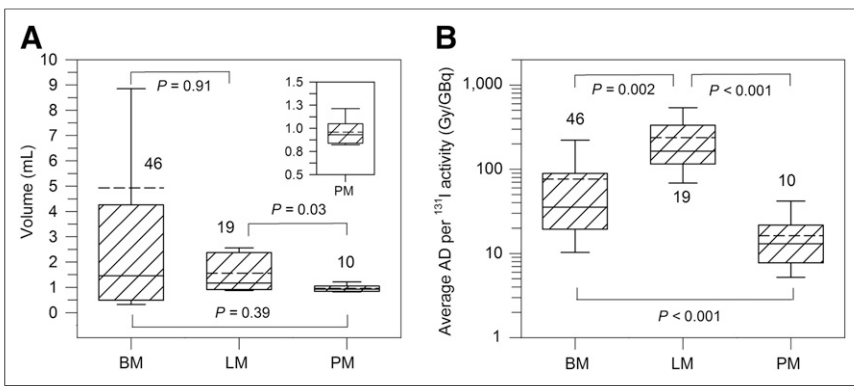


**FIGURE 1.** Box plots of volumes (A) and average ADs per unit of  $^{131}\text{I}$  activity (B) in known-volume (first) group. Inset is enlarged view of PM volumes. Significant differences were characterized by  $P$  value below 0.05. Number shown close to whiskers is number of lesions. Data for LMs and PMs were retrieved from Jentzen et al. (3). Solid and dashed lines indicate median and mean values, respectively.

In accord with a previous study (3), for  $^{18}\text{F}$ -FDG-negative BMs only, the percentage decrease in 24-h  $^{124}\text{I}$  uptake between pretherapy and follow-up PET was used as a quantitative measure of therapeutic efficacy and is referred to as the response index. A response index of 100% denotes a completely responding BM, whereas a value of less than 100% denotes an incompletely responding BM. The response rate at different AD thresholds starting at 85 Gy was determined and was expressed as the percentage of completely responding BMs above the respective AD threshold.

#### Visual Assessment of Nonuniformity

For the large-volume group, 5 nuclear medicine specialists visually assessed the nonuniform radioiodine activity distribution within the segmented BM volume of interest. A 3-point scale was applied: score 0, none; score 1, uncertain; and score 2, substantial. The individual scores of each observer were summed and divided (or normalized) by the highest achievable score (of 10). A BM was assigned to be clearly nonuniform or uniform if the normalized score threshold was at least 0.8 or no more than 0.2, respectively. The normalized score thresholds were derived by statistical simulation, representing a probability of about 9% that the respective values could be obtained by chance.

#### Statistics

The descriptive statistics included the mean, median, SD, minimum, and maximum. Differences between 2 groups were evaluated by the Mann–Whitney  $U$  test. A  $P$  level of less than 0.05 was considered to be statistically significant.

#### RESULTS

##### Patient Characteristics

Ten patients (8 female and 2 male) met the inclusion criteria. There were 5 patients with papillary differentiated thyroid cancer and 5 patients with follicular differentiated thyroid cancer. Stimulation of TSH ( $\geq 30$  mIU/mL) was achieved endogenously in 9 patients before therapy and 7 patients on follow-up and exogenously in 1 patient before therapy and 3 patients on follow-up. Therapeutic activities greater than 11 GBq were administered to 2 patients. The descriptive statistics yielded the following values: mean age  $\pm$  SD,  $63 \pm 13$  y (median, 64 y; range, 42–78 y); mean pretherapy and posttherapy  $^{124}\text{I}$  activity,  $25 \pm 5$  MBq (median, 23 MBq; range, 22–43 MBq); mean single therapeutic  $^{131}\text{I}$  activity,  $8 \pm 5$  GBq (median, 6 GBq; range, 1–20 GBq); and mean follow-up time,  $8.0 \pm 5.9$  mo (median, 5.9 mo, range, 3.7–23.2 mo).

##### Characteristics of BMs

In total, 61 BMs in the 10 patients were included, of which 46 (75%) and 15 (25%) comprised the known-volume group and the fixed-volume group, respectively. The BMs were located in the following body regions: vertebra (22 BMs), rib (19 BMs), skull (7 BMs), pelvis (6 BMs), femur (2 BMs), sternum (2 BMs), and 1 BM each in the clavicle, humerus, and scapula. For the known-volume group, the statistics for volume and average AD per  $^{131}\text{I}$  activity are illustrated in Figure 1. The descriptive statistics yielded the following values: mean volume,  $4.93 \pm 13.0$  mL (median, 1.46 mL; range, 0.20–85.3 mL); mean AD per unit of  $^{131}\text{I}$  activity,  $76 \pm 103$  Gy/GBq (median, 36 Gy/GBq; range, 5–577 Gy/GBq); and mean AD in therapy,  $388 \pm 586$  Gy (median, 183 Gy; range, 39–3,560 Gy). For the fixed-volume group, the minimum AD per unit of  $^{131}\text{I}$  activity

was  $94 \pm 85$  Gy/GBq (median, 63 Gy/GBq; range, 21–270 Gy/GBq), and the minimum AD in therapy was  $489 \pm 423$  Gy (median, 270 Gy; range, 63–1,270 Gy).

For comparison, the respective statistics for 20 LMs and 10 PMs (all known volumes) from a previous study (3) are illustrated in Figures 1 and 2. BM volumes were, on average, larger than for other metastatic tissue types but not to a statistically significant degree (Fig. 1A). The median AD per unit of  $^{131}\text{I}$  activity for BMs was significantly lower, almost by a factor of 5 (36 Gy/GBq vs. 165 Gy/GBq), than for LMs (Fig. 1B,  $P = 0.002$ ). A significantly smaller median AD per unit of  $^{131}\text{I}$  activity was found for PMs (13 Gy/GBq) relative to BMs ( $P < 0.001$ ). The half-lives are illustrated in Figure 2A. The median half-life tended to

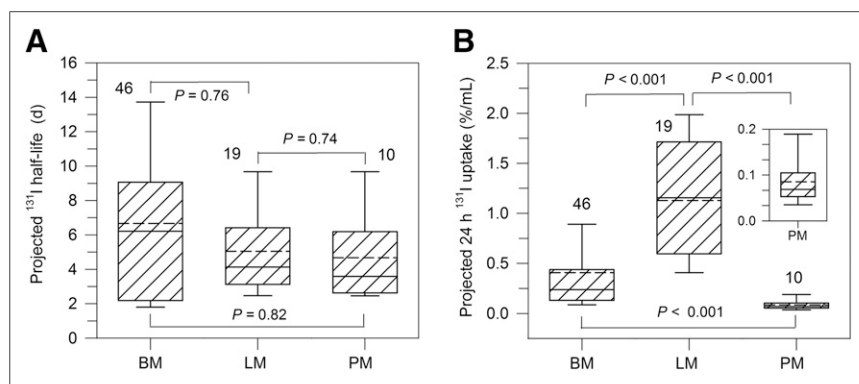


**FIGURE 2.** Box plots of projected  $^{131}\text{I}$  half-lives (A) and projected  $^{131}\text{I}$  24-h uptake values per milliliter (B) in known-volume (first) group. Inset is enlarged view of PM uptake values per milliliter. Significant differences were characterized by  $P$  value below 0.05. Number shown close to whiskers is number of lesions. Data for LMs and PMs were retrieved from Jentzen et al. (3). Solid and dashed lines indicate median and mean values, respectively.

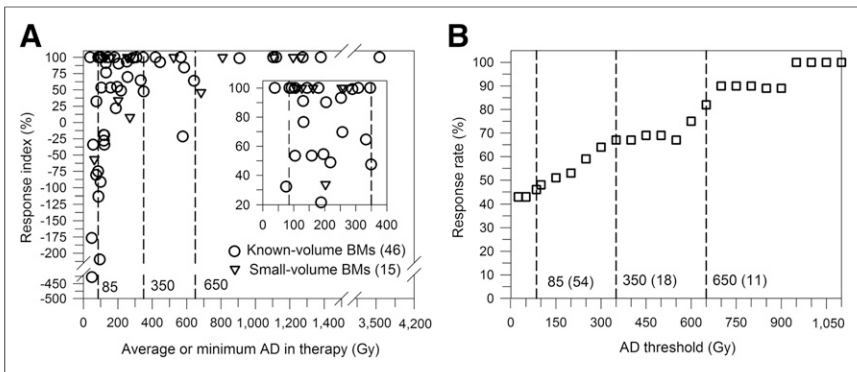


**FIGURE 3.** Dose-response diagram of known-volume and fixed-volume groups (A) and resulting response rate as function of AD threshold (B). Inset is enlarged view of region with high data-point density. Vertical dashed lines indicate AD threshold value for LMs (85 Gy) and AD threshold range for BMs (350–650 Gy). Numbers within parentheses are numbers of BMs included.

be higher in BMs (6.2 d) than in LMs (4.1 d) or PMs (3.6 d), but the difference was not statistically significant. The lowest median 24-h  $^{131}\text{I}$  uptake/mL (Fig. 2B) was observed for BMs (0.24%/mL) and PMs (0.07%/mL). The highest median 24-h  $^{131}\text{I}$  uptake/mL was found for LMs (1.16%/mL) and was 5 times higher than that for BMs ( $P < 0.001$ ).

#### Dose Response and Response Rate

Figure 3A illustrates the dose-response diagram of the known-volume and fixed-volume groups. Of the 61 BMs, more than half (35) responded incompletely (31 of the known-volume and 4 of the fixed-volume group). The percentage of incompletely responding BMs with response indices greater than 90% was 17% (6/35). More than one third (14/35) of the incompletely responding BMs had negative response indices, indicating higher  $^{124}\text{I}$  uptake in follow-up than in pretherapy PET. In a patient-based assessment, a complete BM response was observed for 3 patients; each had only 1 BM. None of the BMs showed a significant  $^{18}\text{F}$ -FDG uptake on follow-up imaging, thus excluding iodine-negative tumor progress (due to dedifferentiation).

The response rates at different AD thresholds are illustrated in Figure 3B. They were calculated by including both the known-volume and the fixed-volume groups. An AD threshold of 85 Gy resulted in a response rate of 46%. This value was obtained from a total number of 54 BMs, of which 40 belonged to the known-volume group and 14 to the fixed-volume group. A response rate

of 82% was ascertained at an AD threshold of 650 Gy, which was obtained from 11 BMs (6 known-volume BMs, 5 fixed-volume BMs). A slightly lower response rate of 67% derived from 18 BMs (12 known-volume BMs, 6 fixed-volume BMs) was obtained at an AD threshold of approximately 350 Gy. A response rate range of 70%–80% was achieved at an AD threshold range of 350–650 Gy. The percentage of completely responding BMs within 4 groups of ADs defined by <85 Gy, 85–350 Gy, 350–650 Gy, and >650 Gy were 14% (1/7), 36% (13/36), 43% (3/7), and 82% (9/11), respectively.

The follow-up time statistics yielded a mean of  $7.3 \pm 5.3$  mo (median, 5.6 mo; range, 3.7–23.2 mo) for the group of incompletely responding BMs and a mean of  $6.3 \pm 3.8$  mo (median, 5.6 mo; range, 3.7–23.2 mo) for the group of completely responding BMs. No statistically significant difference in the median follow-up time between the 2 groups was found ( $P = 0.40$ ).

Two thirds of BMs (39/61) in 7 patients were assessed after a follow-up time greater than 5 mo; the follow-up time was below 4 mo for only 1 patient with a total of 8 BMs, of which 5 responded completely and 3 responded incompletely (range of response indices, 84%–99%).

#### Nonuniformity

There were 26 BMs that were amenable to visual assessment of nonuniformity (Fig. 4). Only one quarter (7/26) responded completely and almost three quarters (17/26) were scored as clearly nonuniform. Of these clearly nonuniform BMs, two thirds (11/17) responded incompletely. If the large BMs received less than 650 Gy, only one fifth (5/23) responded completely. Three clearly nonuniform BMs showed a complete response (2 BMs) or very high response (1 BM, response index of 99%) if they received an AD above 900 Gy. Six BMs were scored as clearly uniform, of which 5 BMs responded incompletely.

#### DISCUSSION

After application of dosimetry-guided  $^{131}\text{I}$  activities, more than half of the BMs (35/61) were still evident on follow-up  $^{124}\text{I}$  PET. Approximately one third (14 BMs) of the 35 incompletely responding BMs showed increased radioiodine uptake after treatment, indicating progressive or at least stable disease. Such an insufficient patient-basis response of BMs was also observed in the standard-activity approach (6–8). One study (6), however, reported complete disease remission after single standard  $^{131}\text{I}$  activities of 3.7–11.1 GBq in 3 patients, each of whom had 3 or fewer BMs. Likewise, in the present study, after administration of 6–8 GBq BMs were not evident in 3 patients, each of whom had borne 1 small BM (volume  $\leq 0.3$  mL). The observed incomplete lesion-based response of BMs is in contrast to the high therapeutic efficacy in other sites. A recent dosimetry-guided  $^{124}\text{I}$  PET

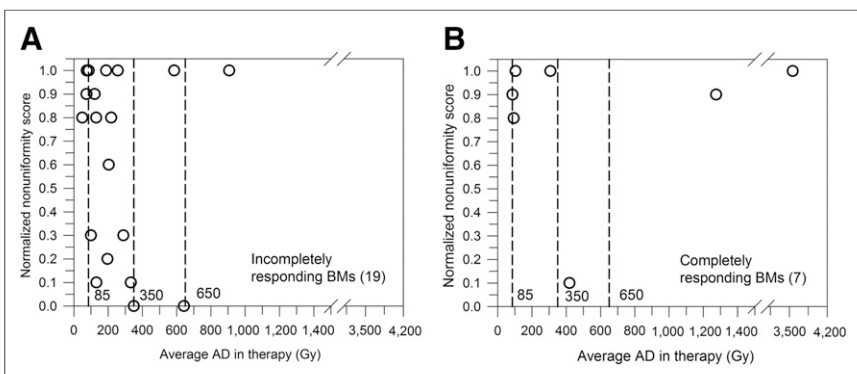


**FIGURE 4.** Relationship between normalized nonuniformity score and average delivered AD for incompletely (A) and completely (B) responding BMs in large-volume group. Vertical dashed lines indicate AD threshold value for LMs (85 Gy) and AD threshold range for BMs (350–650 Gy).

response study (3) of our group using a patient cohort different from that in the present study demonstrated that more than three quarters of LMs (66/84) and almost all PMs (33/34) were not evident on follow-up  $^{124}\text{I}$  PET images after a single  $^{131}\text{I}$  administration.

Hence, both the standard-activity approach and even the dosimetry-guided approach often fail to achieve high therapeutic efficacy for patients with BMs when a single therapeutic activity is administered. In a framework of a lesion-based response analysis, there are two main reasons for this finding.

First, the average AD threshold of approximately 85 Gy—deemed sufficient for achieving a high response by soft tissue and metastatic tissue—appears to be too low for BMs. As illustrated in Figure 3A, an AD threshold of 85 Gy produces a complete response in less than half the BMs. This finding provides evidence that, in BMs, an AD threshold of 85 Gy is too low to achieve high therapeutic efficacy. From Figure 3B, it can be derived that a response rate range of 70%–80% was achieved at an AD threshold range of 350–650 Gy, a value that is almost 4–8 times higher than that for LMs.

We surmise that this high AD threshold range is not caused by such factors as a difference in radiosensitivity between BM and LM tissues but rather results primarily from distinct levels of spatial nonuniformity in ADs, indicating that the average AD may not be a suitable response quantity (16). This hypothesis is substantiated by several observations. There is a great variation in individual BM response in an AD range of 85–650 Gy (Fig. 3A) that may be partly explained by distinct levels of nonuniform uptake (17). In addition, because BMs are generally larger than LMs or PMs (Fig. 1A), nonuniform uptake is more likely in BMs, producing a spatial nonuniformity in ADs. In this study, 26 BMs amenable to visual assessment of nonuniformity were included (large-volume group). Of these, almost three quarters were scored as clearly nonuniform and most of these nonuniform BMs responded incompletely (Fig. 4). This finding demonstrates that most of the large BMs are indeed nonuniform and are therefore difficult to treat effectively, unless the average AD is considerably high. For example, the response rate of clearly nonuniform BMs with an AD of less than 650 Gy was approximately 30% (4/14) (Fig. 4). When the average AD was sufficiently high, 2 clearly nonuniform BMs with an average AD above 1,200 Gy responded completely. The present study did not provide conclusive evidence that nonuniformity at a macroscopic level is the main reason for the insufficient BM response because 5 of 6 BMs visually scored as uniform also responded incompletely (Fig. 4). Finally, compared with soft tissue, osseous tissue has a higher tissue density and therefore has a higher attenuation for  $\beta$ -particles, the dominant radiation mediating the therapeutic response. As a result, the average  $\beta$ -particle range is reduced and the cross-firing contribution is less in osseous than in soft tissue, making BM response more sensitive to nonuniform uptake than soft-tissue response. Further studies are warranted to assess the spatial nonuniformity in ADs at the microscopic and macroscopic levels using sophisticated approaches (18–20).

The second key factor making radioiodine therapy less effective is the finding that BMs have, on average, a significantly lower AD per unit of  $^{131}\text{I}$  activity than LMs (Fig. 1B,  $P < 0.002$ ). An approximately 5 times higher amount of  $^{131}\text{I}$  activity is required to achieve an equivalent median AD for BMs. A closer inspection revealed that the difference in AD per unit of  $^{131}\text{I}$  activity was primarily caused by a significantly lower 24-h uptake per milliliter

for BMs relative to LMs (Fig. 2,  $P < 0.001$ ), rather than their effective  $^{131}\text{I}$  half-lives. For PMs, a significantly lower median AD per unit of  $^{131}\text{I}$  activity relative to BMs was observed; however, the comparison is hampered because of the low number of PMs included and, in particular, because of respiratory motion, resulting in seemingly lower ADs per unit of  $^{131}\text{I}$  activity for PMs (3,21). Consequently, the significant difference in the AD per unit of  $^{131}\text{I}$  activity (and the 24-h  $^{131}\text{I}$  uptake) between BMs and PMs is probably only seemingly apparent; further studies using respiratory gating techniques are warranted (22).

Several limitations are worth noting. The AD threshold range of 350–650 Gy relied on 18 BMs, and therefore, a validation study is necessary (Fig. 3B). Moreover, because of the inclusion and exclusion criteria for patients and for BMs, only 10 patients were enrolled. In addition, one third (20/61) of the BMs showed slow kinetics; their projected effective  $^{131}\text{I}$  half-lives were greater than the physical  $^{131}\text{I}$  half-life, and therefore, their ADs may be somewhat overestimated because physical  $^{131}\text{I}$  decay was assumed after the last measured uptake point. Furthermore, the ADs for rib metastases (approximately one third of the total BMs) may be underestimated because of respiratory motion (3,21). Finally, we cannot rule out that in the case of thyroid hormone withdrawal a further increasing TSH level after the  $\geq 96$ -h period of pretherapy imaging may have modified the predicted AD in therapy. In consequence, the predicted AD may be underestimated if radioiodine therapy is performed after pretherapy dosimetry. However, this effect may be marginal because a pretherapy TSH stimulation level of at least 30 mIU/L, which is considered adequate, was achieved in all patients.

## CONCLUSION

Both the high AD threshold associated with high response rates and the low median AD per unit of  $^{131}\text{I}$  activity contribute to the difficulty in achieving therapeutic efficacy for BMs when a single standard activity is administered. This finding agrees with clinically well-established experience. The relatively high AD threshold range is most likely a result of distinct levels of spatial nonuniformity in ADs. Further studies are warranted to assess the spatial nonuniformity in ADs at the microscopic level. For differentiated thyroid cancer patients with potential BMs, individual patient  $^{124}\text{I}$  dosimetry may be especially important to increase therapeutic efficacy and to predict therapy failure.

## DISCLOSURE

The costs of publication of this article were defrayed in part by the payment of page charges. Therefore, and solely to indicate this fact, this article is hereby marked “advertisement” in accordance with 18 USC section 1734. No potential conflict of interest relevant to this article was reported.

## REFERENCES

1. Luster M, Clarke SE, Dietlein M, et al. Guidelines for radioiodine therapy of differentiated thyroid cancer. *Eur J Nucl Med Mol Imaging*. 2008;35:1941–1959.
2. Haugen BR, Alexander EK, Bible KC, et al. American Thyroid Association management guidelines for adult patients with thyroid nodules and differentiated thyroid cancer. *Thyroid*. 2016;26:1–133.
3. Jentzen W, Hoppenbrouwers J, van Leeuwen P, et al. Assessment of lesion response in the initial radioiodine treatment of differentiated thyroid cancer using  $^{124}\text{I}$  PET imaging. *J Nucl Med*. 2014;55:1759–1765.

4. Jentzen W, Bockisch A, Ruhlmann M. Assessment of simplified blood dose protocols for the estimation of the maximum tolerable activity in thyroid cancer patients undergoing radioiodine therapy using  $^{124}\text{I}$ . *J Nucl Med*. 2015;56:832–838.
5. Maxon HR, Englaro EE, Thomas SR, et al. Radioiodine-131 therapy for well-differentiated thyroid cancer: quantitative radiation dosimetric approach—outcome and validation in 85 patients. *J Nucl Med*. 1992;33:1132–1136.
6. Petrich T, Widjaja A, Musholt TJ, et al. Outcome after radioiodine therapy in 107 patients with differentiated thyroid carcinoma and initial bone metastases: side-effects and influence of age. *Eur J Nucl Med*. 2001;28:203–208.
7. Hindié E, Zanotti-Fregonara P, Keller I, et al. Bone metastases of differentiated thyroid cancer: impact of early  $^{131}\text{I}$ -based detection on outcome. *Endocr Relat Cancer*. 2007;14:799–807.
8. Qiu ZL, Song HJ, Xu YH, et al. Efficacy and survival analysis of  $^{131}\text{I}$  therapy for bone metastases from differentiated thyroid cancer. *J Clin Endocrinol Metab*. 2011;96:3078–3086.
9. O’Connell ME, Flower MA, Hinton PJ, et al. Radiation dose assessment in radioiodine therapy: dose-response relationships in differentiated thyroid carcinoma using quantitative scanning and PET. *Radiother Oncol*. 1993;28:16–26.
10. Freudenberg LS, Jentzen W, Görge R, et al.  $^{124}\text{I}$ -PET dosimetry in advanced differentiated thyroid cancer: therapeutic impact. *Nuklearmedizin*. 2007;46:121–128.
11. Jentzen W. An improved iterative thresholding method to delineate PET volumes using the delineation-averaged signal instead of the enclosed maximum signal. *J Nucl Med Technol*. 2015;43:28–35.
12. Jentzen W, Freudenberg L, Bockisch A. Quantitative imaging of  $^{124}\text{I}$  with PET/CT in pretherapy lesion dosimetry: effects impairing image quantification and their corrections. *Q J Nucl Med Mol Imaging*. 2011;55:21–43.
13. Jentzen W, Hobbs R, Stahl A, et al. Pre-therapeutic iodine-124 PET(CT) dosimetry confirms low average absorbed doses per administered iodine-131 activity to the salivary glands in radioiodine therapy of differentiated thyroid cancer. *Eur J Nucl Med Mol Imaging*. 2010;37:884–895.
14. Jentzen W, Freudenberg L, Eising EG, et al. Optimized  $^{124}\text{I}$  PET dosimetry protocol for radioiodine therapy of differentiated thyroid cancer. *J Nucl Med*. 2008;49:1017–1023.
15. McDougall IR, Iagaru A. Thyroid stunning: fact or fiction? *Semin Nucl Med*. 2011;41:105–112.
16. Neti PV, Howell RW. When may a nonuniform distribution of  $^{131}\text{I}$  be considered uniform? An experimental basis for multicellular dosimetry. *J Nucl Med*. 2003;44:2019–2026.
17. Dorn R, Kopp J, Vogt H, et al. Dosimetry-guided radioactive iodine treatment in patients with metastatic differentiated thyroid cancer: largest safe dose using a risk-adapted approach. *J Nucl Med*. 2003;44:451–456.
18. Hindié E, Champion C, Zanotti-Fregonara P, et al. Calculation of electron dose to target cells in a complex environment by Monte Carlo code “CELDOSE.” *Eur J Nucl Med Mol Imaging*. 2009;36:130–136.
19. Vaziri B, Wu H, Dhawan AP, et al. MIRD pamphlet no. 25: MIRDcell V2.0 software tool for dosimetric analysis of biologic response of multicellular populations. *J Nucl Med*. 2014;55:1557–1564.
20. Sgouros G, Hobbs RF, Atkins FB, et al. Three-dimensional radiobiological dosimetry (3D-RD) with  $^{124}\text{I}$  PET for  $^{131}\text{I}$  therapy of thyroid cancer. *Eur J Nucl Med Mol Imaging*. 2011;38(suppl 1):S41–S47.
21. Pevsner A, Nehmeh SA, Humm JL, et al. Effect of motion on tracer activity determination in CT attenuation corrected PET images: a lung phantom study. *Med Phys*. 2005;32:2358–2362.
22. Pépin A, Daouk J, Bailly P, et al. Management of respiratory motion in PET/computed tomography: the state of the art. *Nucl Med Commun*. 2014;35:113–122.